High-speed imaging of non-photochemical laser-induced nucleation in aqueous cesium chloride

Eleanor R. Barber and Andrew J. Alexander*

School of Chemistry, University of Edinburgh, David Brewster Road, Edinburgh, EH9 3FJ

**e-mail: andrew.alexander@ed.ac.uk*

SI1. Experimental details

Sample cooling and supersaturation

The method of cooling depended on the sample concentration. The 11.9 mol kg^{-1} samples were cooled in air for two hours to 25 °C, then transferred to a water bath at the target temperature approximately half an hour before use. Since the 13.1 mol kg^{-1} samples were liable to spontaneously nucleate if disturbed during cooling, they were transferred whilst hot to the location of the water bath within a polystyrene box. The vials were then left to cool inside the box for 75 minutes, the final 25 minutes with the box lid removed. The vials were transferred to the water bath 45 minutes before use. The resulting supersaturations achieved are given in **Table S1**, calculated using tabulated solubility data.[1]

Concentration (*C*) / mol kg^{-1}	**Temperature (*T*) / °C**	**Supersaturation (*S*)**
11.9	25	1.05
11.9	21	1.07
13.1	21	1.18

Table S1. Summary of experimental solution concentrations, temperatures and resulting supersaturations of samples.[1]

Imaging experiments

A schematic diagram of the two directions used for imaging are shown in **Fig. S1**. For illumination with the low-speed digital camera, a continuous-wave (CW) laser beam with wavelength of 488 nm was used. When imaging from the front, a cross-section of the beam path at the incident location of the pulse was visible. When imaging from the side position, the entire beam path through the vial from the entry to exit was visible. With the high-speed camera, samples were imaged from the side only. For illumination with the high-speed camera, a bright white light-emitting diode (LED) was used, positioned at an angle or directly into the camera (**Fig. S2**).

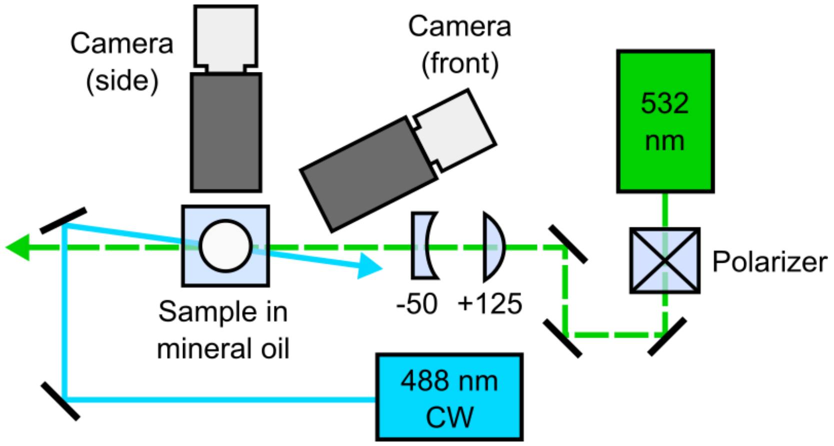

Fig. S1. Schematic diagram of the optical setup and the two different camera positions used for imaging with the low-speed digital camera. The 488-nm CW laser passed through the centre of the sample vial, entering at the opposite side and at a shallow angle to the laser pulse (532 nm) used for NPLIN.

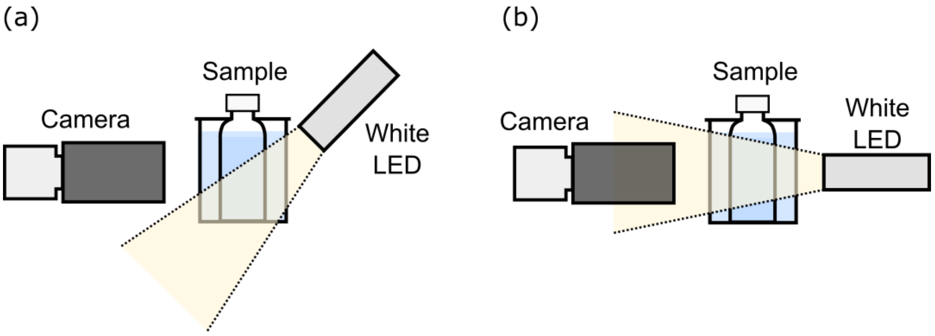

Fig. S2. The two different angles of the LED used for lighting when imaging with the high-speed camera. (a) At lower frame rates, the LED was angled downwards so that the crystals appeared as white particles against a black background. (b) At higher frame rates, the LED was shone directly into the camera so that the crystals appeared as black particles against a light grey background.

The framerate of both cameras could be increased by decreasing the vertical dimension of the images. The exposure time was always set to the maximum value at a given frame rate, in order to minimise dead time between frames. As the frame rate increases and the exposure time decreases, more light is required for imaging. The small size of the images at very high frame rates also limits the usefulness of the results, so a balance between frame rate and imaging quality was required. For the standard digital camera, the highest frame rate used to record images was 700 fps.

The high-speed camera had a selection of preset frame rates, ranging from 1000 fps to 675,000 fps. At lower frame rates (up to 54,000 fps) sufficient lighting was obtained when the LED was angled downwards (**Fig. S2(a)**) so that it was not shining directly into the camera. The crystals were visible as white particles against a black background in the resulting images. At higher frame rates, more light was required, and the LED was angled so that it shone directly at the camera (**Fig. S2(b)**). The highest frame rate used to record images with the high-speed camera was 250,000 fps.

The perspective when viewing samples from the front position with the low-speed camera is illustrated schematically in **Fig. S3**, which corresponds to the images shown in **Fig. 2** of the main article.

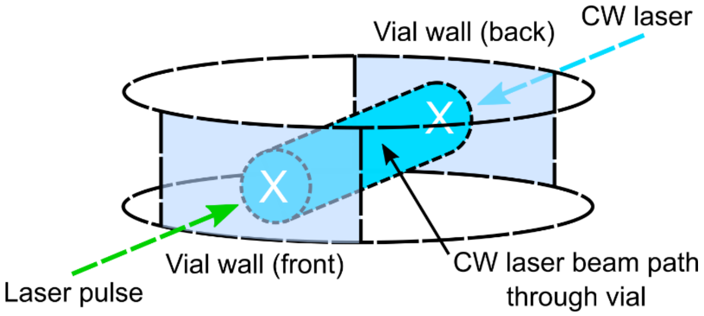

Fig. S3. Schematic diagram (not to scale) showing the perspective when viewing samples from the front position. The areas marked ‘X’ appear as bright spots in images and correspond to the entry and exit points of the CW beam. The diameter of the pulsed laser is not shown but is approximately four times larger than the CW laser, so crystals will also form outside of the CW beam path.

Imaging of crystals on millisecond timescale

Table S2 shows the earliest times that growing particles (eventually identified as crystals) were observed in both the bulk solution and on the vial inner walls using the low-speed camera. As the frame rate was increased, the image height had to be reduced, making it more difficult to capture random nucleation events in focus.

Image height / pixels	**Frame rate / fps**	**Exposure time / µs**	**Time first crystal seen / ms**	
			Bulk solution	**Vial walls**
400	250	3864	3.9	3.9
60	600	1526	22.6	1.5
20	700	1288	28.3	1.3

Table S2. Table summarising the earliest times that cesium chloride crystals were observed, in the bulk solution or on the inside of the vial walls, in supersaturated aqueous solution ($C = 11.9$ mol kg^{-1}, $S = 1.05$) following NPLIN. The incident laser pulse (5.0 ns, 532 nm) had an energy density of 920 mJ cm^{-2}.

Fluctuations in brightness

Fig. S4 illustrates growth of crystals observed using the low-speed camera (250 fps) imaged from the side position. The arrow indicates a crystal is observed during the same frame in which the NPLIN laser pulse occurs. By 36 ms this particle shows structure consistent with the star shaped habit of the resulting CsCl crystals. This figure also illustrates a crystal with fluctuating intensity (highlighted by the white square). The fluctuation in brightness was attributed to the imaging setup, possibly due to the illuminating light source.

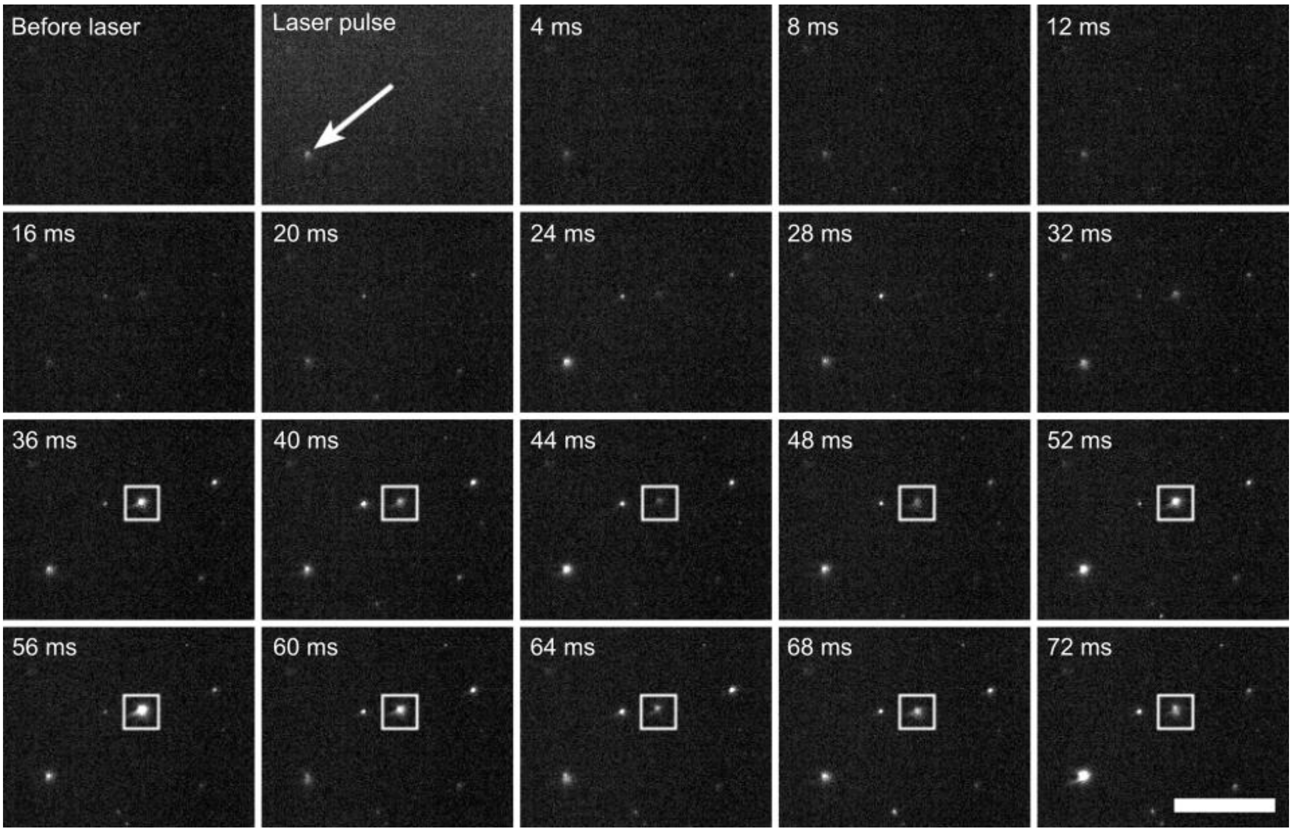

Fig. S4. Growth of cesium chloride crystals from a supersaturated aqueous solution (C = 11.9 mol kg^{-1}, S = 1.05) following NPLIN. The incident laser pulse (5.0 ns, 532 nm) had an energy density of 920 mJ cm^{-2}. Consecutively recorded images are shown, starting from top left, with a frame rate of 250 fps and an exposure time of 3.9 ms. A crystal is observed in the same frame as the laser pulse (white arrow). In this frame, the laser pulse itself is also faintly visible as a lightening of the dark background. The crystal highlighted by the white box fluctuates in brightness from frame to frame, which is artifact of the imaging setup. Brightness and contrast levels have been optimised for clarity. Scale bar represents 500 μm.

Measurements of minimum grey value

It should be noted that measuring the area of the crystals was not effective because they were visible only as a single pixel at the early stages of growth. For example, for the S = 1.18 data (**Fig. 6**) the minimum grey value steadily decreases from approximately 160 to 145 in the 17 ms following the laser pulse, during which time the size of the crystal in the corresponding images increases only from 1 to 2 pixels.

References

1 D. Lide, Ed., *CRC Handbook of Chemistry and Physics, 86th Edition*, CRC Press, Boca Raton, FL, 2005.